CrossMark

ORIGINAL

Experimental investigation of the effect of air velocity on a unit cooler under frosting condition: a case study

Ergin Bayrak[1] · Akın Çağlayan[2] · Alp Er S. Konukman[1]

Abstract Finned tube evaporators are used in a wide range of applications such as commercial and industrial cold/freezed storage rooms with high traffic loading under frosting conditions. In this case study, an evaporator with an integrated fan was manufactured and tested under frosting conditions by only changing the air flow rate in an ambient balanced type test laboratory compared to testing in a wind tunnel with a more uniform flow distribution in order to detect the effect of air flow rate on frosting. During the test, operation was performed separately based on three different air flow rates. The parameters concerning test operation such as the changes of air temperature, air relative humidity, surface temperature, air-side pressure drop and refrigerant side capacity etc. were followed in detail for each air flow rate. At the same time, digital images were captured in front of the evaporator; thus, frost thicknesses and blockage ratios at the course of fan stall were determined by using an image-processing technique. Consequently, the test and visual results showed that the trendline of air-side pressure drop increased slowly at the first stage of test operations, then increased linearly up to a top point and then the linearity was disrupted instantly. This point speculated the beginning of defrost operation for each case. In addition, despite detecting a velocity that needs to be avoided, a test applied at minimum air velocity is superior to providing minimum capacity in terms of loss of capacity during test operations.

✉ Alp Er S. Konukman
konukman@gtu.edu.tr

[1] Department of Mechanical Engineering, Energy Systems Division, Gebze Technical University, 41400 Gebze, Kocaeli, Turkey

[2] Research and Development Department, Friterm Inc., 34957 Istanbul, Turkey

List of symbols
BR   Blockage ratio (%)
D   Diameter (mm)
EXV   Electronic expansion valve (−)
FP   Fin pitch (mm)
FT   Fin thickness without frost (mm)
TT   Total tube thickness with frost (mm)
L   Length (mm)
RH   Relative humidity (%)
T   Temperature (°C)
TXV   Thermostatic expansion valve (−)
X   Transversal pitch (mm)

Greek symbols
δ   Frost thickness (mm)

Subscript
a   Air
ai   Air inlet
evap Evaporation
f   Fin
g   Gap
m   Minute
o   Outlet
s   Surface
sh   Superheat
t   Tube

1 Introduction

Frost formation and its growth are undesirable but unavoidable phenomena in many applications such as cold storage unit coolers and heat pumps. These phenomena lead to a decrease of heat transfer rate caused by the combined effect

of thermal resistance of frost and an increase in air pressure drop. In order to protect the foods against temperature and humidity fluctuations in the room, a periodic defrost process is carried out at suitable time intervals for the sake of balanced energy efficiency and food protection. However, the parameters which have a significant impact on frost growth should be exactly clarified to detect optimum time of defrost period.

As can be seen in the literature, the effects of air flow rate on frost formation and growth is still unclear and there are some conflicts among researches; besides, there is not enough experimental and visual data regarding unit coolers tested with casing and fans integrated like in real operating conditions. The previous studies generally dealt with investigations under constant air flow conditions.

Author such as Chen et al. [1], Aljuwayhel et al. [2], Schmidt and Kristensen [3], Da Silva [4], Huang et al. [5] and Groll et al. [6] investigated frost growth on tube-finned evaporators under variable air flow conditions. While these studies have highlighted the change of heat transfer rate and pressure drop depending on frost formation, some of them have examined the effects of fan types on frost growth.

Yan et al. [7], Cui et al. [8], Padhmanabhan et al. [9] claimed that the amount of frost formation increases as air flow rate decreases. This is because the surface of the heat exchanger becomes colder for a lower flow rate due to a lower heat transfer rate. If examined in detail, Yan et al. [7] investigated the effects of various parameters such as relative humidity, fin pitch, row number under frosting conditions but our study is going to deal with the effect of air flow rate at the same condition. In this context, they have carried out a test procedure in order to show the effects of air flow rate on heat transfer and pressure drop characteristic of heat exchangers. As a result of this study, frost formation was greater for a lower air flow rate because the surface of heat exchanger was colder. In addition, lower air flow rate causes an increment of pressure drop due to the fact that the more frost formation occurs, the more passage is blocked. In addition, an increase in frosting rate leads to a faster decrease of heat transfer rate and the overall heat transfer coefficient. In another study performed by Cui et al. [8], the performance of fin-and-tube heat exchanger under frost condition was investigated numerically and validated via the analytical method. They found that the amount of frost accumulation increases as the velocity of moist air decreases because the temperature difference between moist air and fins is larger. Thus, the heat exchanger coefficient degrades faster and the pressure drop enlarges significantly. Padhmanabhan et al. [9] have specified that for high air velocities, when the heat transfer coefficient is higher, a higher fin surface temperature and mass transfer coefficient is observed. As the higher fin surface temperature inhibits the frost growth, higher mass transfer

coefficient increases the frost deposition. According to their results, frost thickness decreased at higher velocities. It means that the surface temperature has a more significant impact on frost growth than the mass transfer coefficient.

Contrary to the studies mentioned above, Haijie et al. [10] stated that a simultaneous rise in the mass transfer coefficient and wall temperature increases the frost accumulation rate. Besides, increasing the air flow rate could delay the first occurrence of frosting because fin and tube temperatures increase and the increased air velocity could blow away the frost crystal particles. As a result, the growth rate of frost thickness could be delayed due to appropriate air flow rate; thereby, the defrosting interval can be increased. Moreover, they specified that the frosting rate is not sensitive to the airflow rate because the test results have revealed that the frosting rate is almost the same for different frequencies. This situation is consistent with Da Silva [4] and Tashiro and Hamada [11]. Da Silva [4] conducted a study regarding frost formation, which aims to observe the frost formation phenomenon on the evaporator by the taking into account air flow reduction resulting from frost formation and the thermal–hydraulic performance of evaporators operating under frosting conditions. It has been concluded that the high degree of difference between surface temperature and dew-point temperature decreases the frost density, as the opposite increases the mass transfer rate. Tashiro and Hamada [11] have carried out an experimental study in order to investigate the effects of humidity and the air inlet velocity on frost formation and the dominant factor on frost formation. Taking into account the effects of air velocity in this study, they have concluded that higher inlet velocity reduces the thickness of frost layer because high heat transfer rate makes the frost layer denser although as inlet velocity increases, the frost mass increases as well. Hence, they have specified that the inlet velocity has a considerable effect on the frost density. In addition, they have added that the effect of inlet air velocity has a minor impact on the region of high relative humidity.

The different views on frost formation rate depending on air flow rate are caused by two phenomena: mass transfer coefficient and absolute humidity difference (driving force). According to Ye et al. [12], the situation of frost rate depending on air flow rate could be determined by a dominant factor between these two phenomena. This study also mentions a critical air side heat transfer coefficient phenomenon noticeably affecting frost growth. The relationship between air side heat transfer rate and frost growth is proportional until a point, however later, the opposite happens. This situation results from the tendency of the mass transfer rate to increase or decrease with air velocity and frost growth was determined by the dominant factor relating the change in the mass transfer coefficient and absolute humidity difference.

Within the scope of this case study, the frost formation phenomenon the unit coolers considering the effect of air flow rate was investigated similar to real refrigeration systems. During the test process carried out for different fan frequencies, thereby for different air velocities, all the parameters related to the tests were followed and compared within themselves. The frost thicknesses, blockage ratios and thermal images were detected as well. Consequently, the effect of air flow rate on the unit cooler under real operation conditions was experimentally determined.

2 Test methodology

2.1 Description of the heat exchanger

Table 1 shows the dimensional characteristics of the unit cooler used in this study and pictures have been illustrated in Fig. 1. As stated in Table 1, a plain fin type was selected

Table 1 Geometric parameters of the unit cooler

Geometric parameters	Values
Number of rows	4
Number of circuits	4
Number of tubes per row	22
Transversal tube pitch	35 mm
Longitudinal tube pitch	35 mm
Tube length	745 mm
Tube diameter (inner/outer)	11.86/12.5 mm
Fin thickness	0.15 mm
Fin spacing	7 mm
Fin type	Flat
Fin height	770 mm
Tube arrangement	Inline

for the sake of better visualization and easy measurement of frost formation on fin surface. In addition, the evaporator was equipped with a 500 mm fan with 9500 m^3/h air flow rate.

2.2 Test procedures

The test set-up is illustrated in Fig. 2. The right side of this figure demonstrates the calorimetric room (ambient balanced room) where the test operations were performed. The calorimetric room setup consists of a test section where the fin and tube heat exchanger was installed; an air handling unit in order to maintain constant air temperature and humidity; a refrigeration section to regulate the temperature and flow rate of the refrigerant which was fed to the test unit during the experiments.

The refrigerant used in these experiments was a R404A and the refrigerant system had an auxiliary line, which was operated with water for the purpose of controlling the refrigerant temperature at some parts of the installation such as the condenser subcooling temperature. Besides, this refrigerant line had a shell and tube condenser used for the system's condenser and auxiliary evaporator in order to adjust evaporation pressure.

The type of expansion valve is very important for the frosting test because this apparatus significantly affects the characteristic of the frosting test. An electronic expansion device (EXV) was used in this study. With an EXV expansion device, a better control of the superheat with regard to a TXV is possible and therefore a better usage of the evaporator surface area is possible for steady-state and the frost-up tests [6].
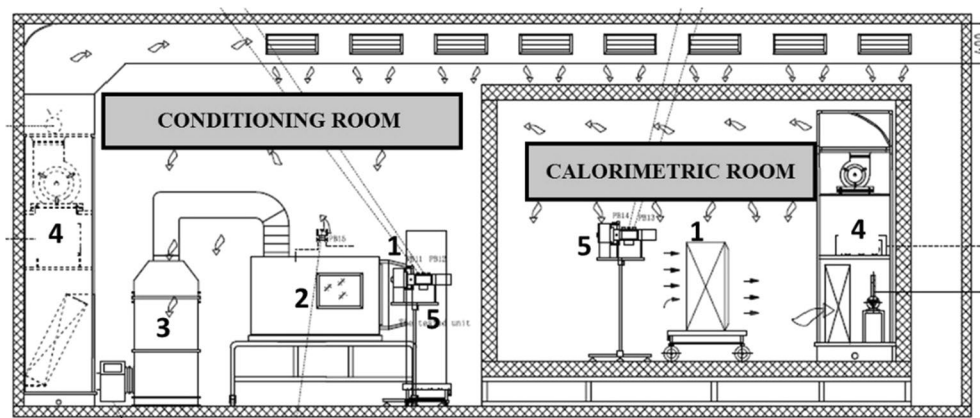
Moreover, while the heat transfer rate of air side was calculated from electrical loads, that of the refrigerant side was calculated from

$$q_{r,tot} = \dot{m}_r \left(h_{r,before\ exp\ valve} - h_{r,o} \right) \tag{1}$$

Fig. 1 The general view of the unit cooler inside the calorimetric room at Friterm R&D laboratory

where, $\dot{m}_r$ is the refrigerant mass flow, $h_{r,before\ exp\ valve}$ and $h_{r,o}$ are enthalpy values of the before expansion valve and the outlet of the refrigerant, respectively. The heat transfer rate of the refrigerant side was taken as the cooling capacity because the uncertainty value of the refrigerant side is smaller when compared with the heat transfer rate of the air side.

During the test operation, while the air inlet temperature was controlled automatically, the relative humidity was controlled manually because the automatic control of relative humidity results in undesirable fluctuations in the wide range. Eventually, a very stable room condition was ensured. On the other hand, the frosting images were taken by a digital camera mounted on a manual traverse mechanism, which was manually able to move from bottom to top.

2.3 Experimental conditions

In scope of this case study, while the air inlet temperature, surface temperature and relative humidity was kept at 3, −9 °C and 77.5% for the entire tests, air initial velocities were 2.52, 3.10 and 3.37 m/s for test numbers of 1, 2 and

3, respectively. The different fan air velocities have been adjusted via a frequency inverter mounted to an axial fan. The superheat temperatures followed during the test operations were about 0.5 °C because it was the desired uniform tube surface temperature in order to evaluate the windward frost thickness and blockage ratio of the unit cooler more accurately.

2.4 Experimental uncertainty

In order to calculate the experimental uncertainty of the related parameters, which result from the accuracy of experimental instruments, the instruments precisions have to be known. These values are shown in Table 2 in detail.

The uncertainty of related parameters was calculated according to Stephanie Bell's 'A Beginners's Guide to Uncertainty of Measurement' [13]. The results are tabulated in Table 3. In order to obtain a good measurement of the frost thickness, it is important that the camera is placed normal to the plane of the coil. Therefore, the camera having a 4224 × 2376 image resolution was mounted on a 2-axis traverse system. In addition, the uncertainty of frost thickness measurement results from two reasons. One of them is

Table 2 Experimental instrument precision

Measurement	Location	Accuracy
Temperature	The refrigerant outlet temperature	±0.1 °C
Temperature	The temperature before expansion valve	±0.1 °C
Temperature	Outlet of circuits	±0.3 °C
Pressure	Evaporation pressure	±0.25%
Refrigerant flow rate	The refrigerant preparation system	±0.6%
Power meter (DPM1)	Fan electrical consumption	±0.1%
Power meter (DPM2)	Total electrical consumption	±0.1%
Step controller	Reading value of ref. flow rate	±0.1%
Step controller	Reading value of ref. pressure	±0.1%
Step controller	Reading value of temperature	±0.3 °C
Static pressure difference (refrigerant)	The inlet and outlet of the product	±0.25%

Table 3 Estimated uncertainty values for the related parameters

Parameters	Maximum uncertainty
Heat transfer rate (kW)	2.35%
Air side static pressure difference (Pa)	0.075%
Pixel in captures	∓1 pixel
Ruler in images	∓0.2 mm
Frost thickness (mm)	∓0.208 mm
Blockage ratio	5.4%

the error from reading the pixel values; the other one is the error of reference meter measurement. The maximum error of reading is about 1 pixel; thereby, the corresponding frost thickness is about 0.06 mm, and the maximum error of reference meter is 0.2 mm. Thus, the overall uncertainty for fin and tube frost thicknesses is about 0.208 mm.

3 Results and discussion

The test process was repeated twice for each test, thus the experimental outcomes were obtained by taking the

average except the air flow rates. The most important parameters during test operation are illustrated in Fig. 3. The first 15 min were spent for the stabilization period in order to reach the desired conditions. After this time, the desired condition for each test was ensured almost constantly during test operations. Moreover, the superheat temperatures during the test stayed stable because of the excellent control of EXV and superior design of the refrigerant distributor.

However, although the control of the relative windward unit cooler humidity was rather difficult, the average value was almost the same as shown in Table 4. The average values of air inlet temperature, superheat temperature and evaporation pressure can also be seen in the same table.

3.1 Frost thickness and blockage ratios

Frost thickness development during the test operation is a rather important phenomenon. It is of vital importance to the system performance due to the fact that the growing frost results in both the decrease of air flow rate and increase in the thermal insulation effect. However, Janssen [14] stated that another reason for the significance
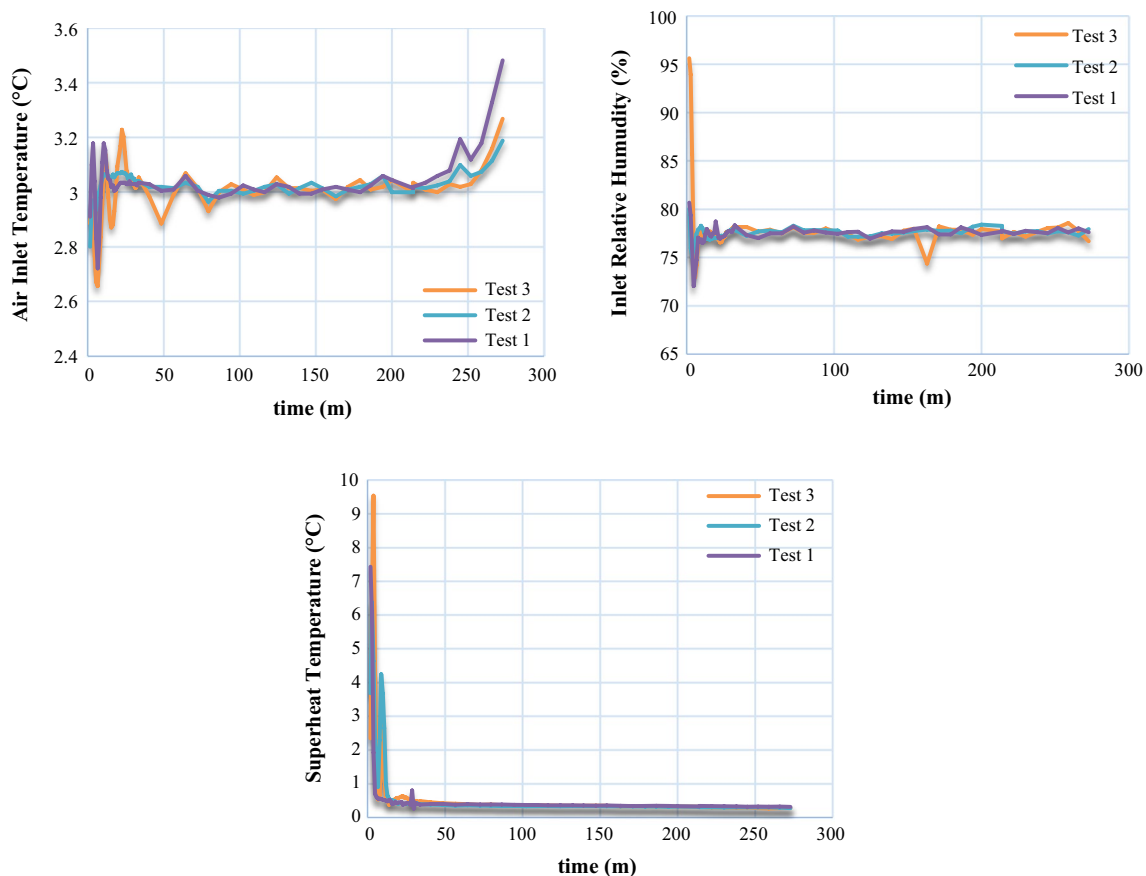

Fig. 3 The changes of air inlet temperature, inlet relative humidity and superheat temperature over time

Table 4 The average values for the test operation

Test	T_{ai} (°C)	RH_{ai} (%)	T_{sh} (°C)	P_{evap} (MPa)
1	3.04	77.53	0.37	0.446
2	3.03	77.50	0.37	0.446
3	3.00	77.44	0.40	0.446

of frost thickness is its direct involvement within the differential equations governing frosting and defrosting, so that researchers need accurate measurement of frost characteristics.

Digital images of frost development with time for Test 3 are shown in Fig. 4 as an example. In the literature, various methods regarding frost measurements are described; visual methods were executed with a camera and image process toolbox or physical measurements were made, for instance using micrometers. In this study, the frost thickness measurements were performed via a visual method because the physical measurements for the

finned tube heat exchanger are quite difficult and are less accurate when compared with visual methods.

First, the images belonging to the specific area of each circuit were captured by a digital camera of 20.4 Megapixel image quality as shown in Fig. 5. Then, the frost thicknesses on both fin and tube were measured for the related areas of each circuit via Matlab Image Processing Toolbox and the average values of frost thickness were taken in order to detect total frost thickness for the related air velocity.

Eventually, the average frost thickness formed at windward of the unit cooler could be obtained at a certain instance when the fan showed instable effects, which is going to be mentioned as the fan stall situation in detail in the next section. As it can be seen in Fig. 6, in order to find the pixel count at per unit length, the imaging equipment was calibrated by means of a reference meter, placed near side the unit cooler. For the fin, the non-frost thickness between the two fins was obtained by taking this reference length; thereby, the frost thickness for the fin was
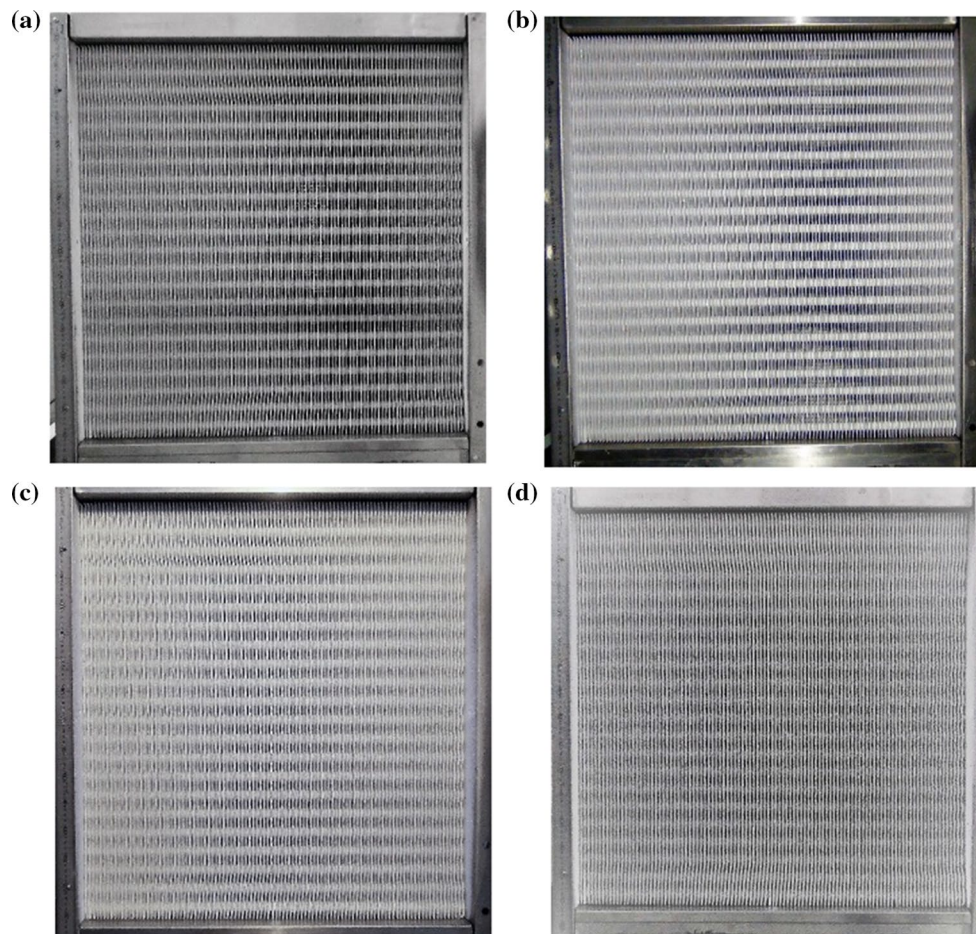
Fig. 4 Digital images of frost development with time in Test 3 at times **a** 77 min. **b** 130 min. **c** 223 min. **d** 277 min
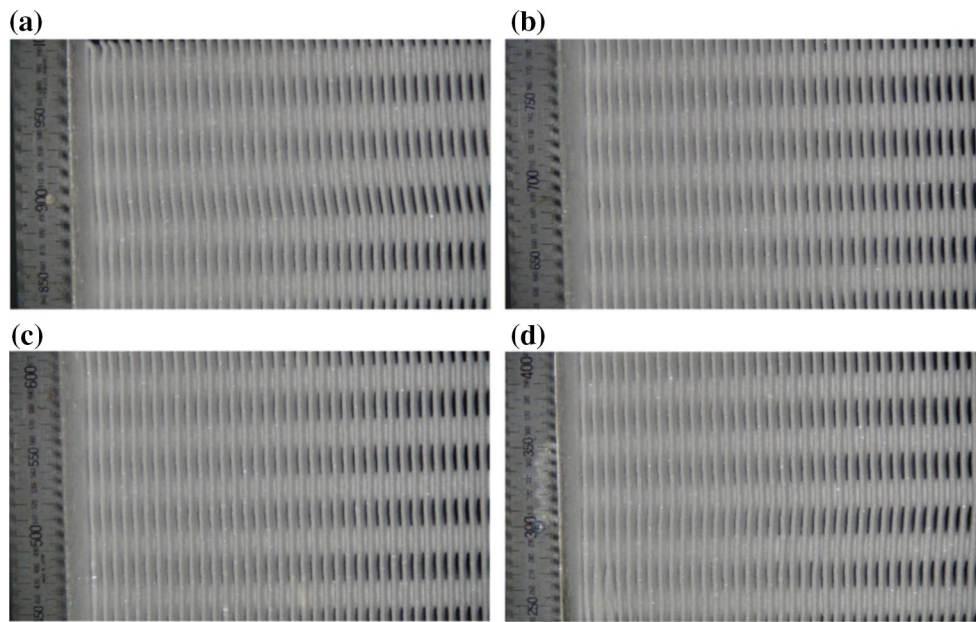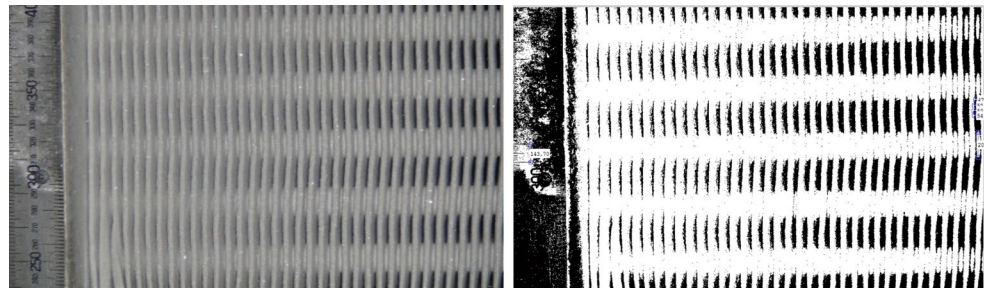
Fig. 5 Images of frost thicknesses for each circuit at 50 Hz test operation at a specific time **a** 1st circuit **b** 2nd circuit **c** 3rd circuit **d** 4th circuit

Fig. 6 Illustration of the digital and post processed images

calculated using the following equation. On the other hand, the tube thickness was directly obtained according to reference length.

$$\delta_f = \frac{(FP - L_g) - FT}{2} \qquad (2)$$

$$\delta_t = \frac{TT - D_o}{2} \qquad (3)$$

At the end of the image analysis, average fin and tube thickness for each test operation was obtained separately. The fin frost thicknesses for the test operations corresponding to number of 1, 2 and 3 were 1.4775, 1.5062 and 1.4506 mm and the tube frost thicknesses were 1.4581, 1.4495 and 1.4729 mm, respectively. (see Table 5 for more details about these values).

Another phenomenon directly related with fin and tube thickness is blockage ratio, which occurs on the windward of the unit cooler, which was evaluated in many studies. According to the following equations, the

blockage ratios of frost for each test operation have been found to be about 50%, which was measured at the beginning of the fan stall, as illustrated in Fig. 7 with uncertainty values and this result is consistent with the study performed by Huang [5]. The author has also stated that the defrost period should start when half of the flow area is blocked by frost. (see Table 5 for blockage ratios).

$$\text{space area}_{\text{non-frost}} = (X_t - D_o) \times (FP - FT) \qquad (4)$$

$$\text{space area}_{\text{after frost}} = (X_t - D_o - 2\delta_t) \times (FP - FT - 2\delta_f) \qquad (5)$$

$$BR\ (\%) = \left(1 - \frac{\text{space area}_{\text{after frost}}}{\text{space area}_{\text{non-frost}}}\right) \times 100 \qquad (6)$$

Another data was taken visually via a microscope in order to observe the shape of the first formation of frost at the starting time of the test operation because some researchers [14] have stated that initial frost formation has a significant impact on further growth of frost.

Table 5 The values of frost thickness and blockage ratios

Circuits	1	2	3	4	AVG
Test 1 (30 Hz)					
Fin side	1.4748	1.5105	1.3891	1.5357	1.4775
Tube side	1.2894	1.5690	1.4172	1.5568	1.4581
Blockage ratio (%)	49.59	51.90	48.05	52.45	50.03
Test 2 (40 Hz)					
Fin side	1.2656	1.4707	1.5259	1.7629	1.5062
Tube side	1.1871	1.4962	1.5547	1.5603	1.4495
Blockage ratio (%)	43.61	50.53	52.22	58.20	51.14
Test 3 (50 Hz)					
Fin side	1.4294	1.4530	1.3878	1.5324	1.4506
Tube side	1.3840	1.5191	1.5783	1.4105	1.4729
Blockage ratio (%)	48.90	50.22	48.87	51.67	49.92
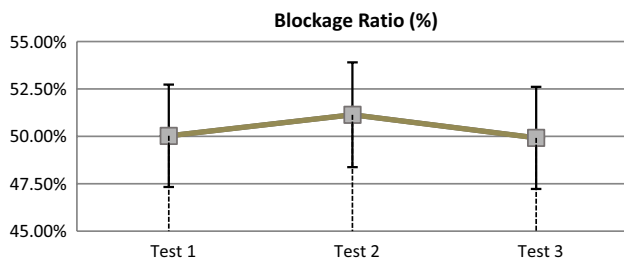
Fig. 7 The blockage ratios for each test operation

Unfortunately, because frost formation occurred in the stabilization period, which occurred 15 min into the experiment, these data could not be obtained.
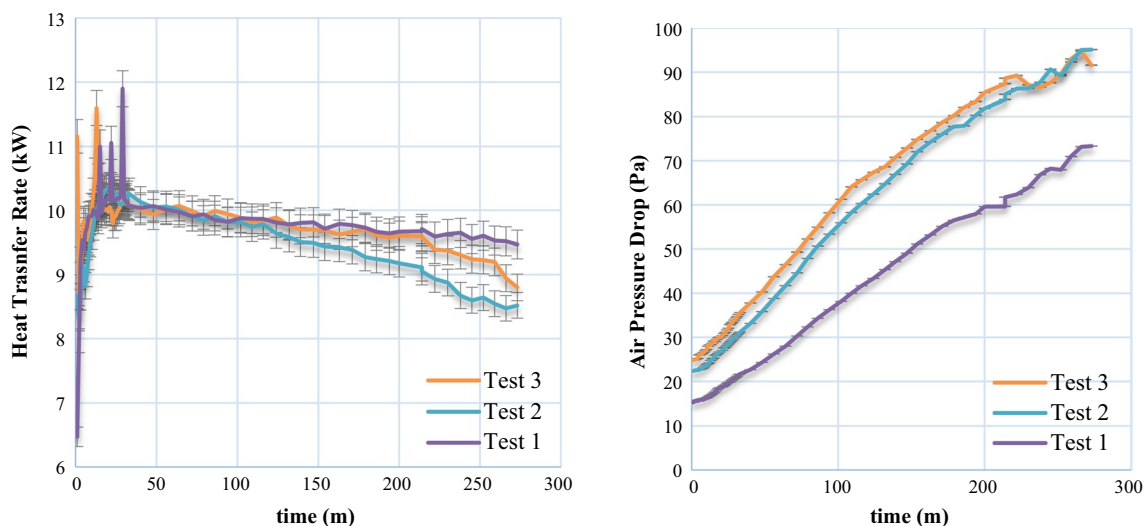
3.2 The change of air-side pressure drop and heat transfer rate

Figure 8 demonstrates the change of air pressure drop and heat transfer rate during the test operation. According to this figure, as the pressure drop slowly increases for the first 40 min, air pressure drop increases steeply after that point, which means that the frost grow rate has increased this time. The interpretation for this situation could be that the amount of frost formation increases as the air flow rate decreases because the surface of the unit cooler becomes colder and the decrease of surface temperature is more dominant when compared with the effect of decrease of the mass transfer coefficient.

Furthermore, while the air pressure drop curve is lower for test 1 as expected, the curves of test 2 and test 3 are very close to each other. However, the augmentation of pressure drop at test 2 is higher than the other values. When examined in detail, considering the heat transfer curves, it can be seen that the heat transfer rate curve for test 2 degrades faster. It may be based on the more effective frost growth at this velocity value than others and this situation could be attributed to the value of critical air velocity for evaporators as highlighted by Ye et al. [12]. In other words, the tendency of the mass transfer rate of frost to increase or decrease depending on air velocity was identified by the dominant factor regarding the change in the mass transfer coefficient and absolute humidity difference (driving force).

According to the same figure, the heat transfer rate decreases continuously. Within the first 110 min, no significant effect of air flow rate on heat transfer rate was observed, after that point, the curve for test 2 decreased

Fig. 8 The change of air-side pressure and heat transfer rate overtime for each test operation

more depending on the aforementioned reasons. In addition, the heat transfer rate for Test 1 and Test 3 were about similar throughout the test operation. Therefore, the running of the fan at 2.52 m/s was the most suitable selection in the scope of this study.

On the other hand, axial fans have a limit for pressure drop. If this limit is exceeded, it could have some detrimental impacts such as an increase in noise and vibration, structural fatigue and the damaging of ductwork and other components. Figure 9, which demonstrates times versus air pressure drops, shows the stall condition for each test operation. The starting point of stall specified with a red circle can speculate the time of the starting point of the defrost process at the frosting tests even when the critical test parameters were stable. Therefore, the blockage ratios were evaluated by taking this limit pressure drop as a point of reference. The interesting point is that this time blockage ratio of the unit cooler surface was about 50% as mentioned in the above section.

4 Conclusion

In this experimental case study, the effect of air flow rate on the unit cooler under frosting condition was observed by using visual methods and image processing. As a conclusion;

- According to the experiments, air velocity has no significant effect on the heat transfer rate for a certain period of time, but it was observed that it gains importance at further times because of the effect of air velocity on frost growth. In addition, as emphasized in other studies, for unit coolers running under frost condition some air velocities need to be avoided. For this study, because the fan air velocity specified as 3.10 m/s should be avoided, the air velocity specified as 2.52 m/s could be a superior point because the product running at this value experiences minimum loss of capacity. This situ-
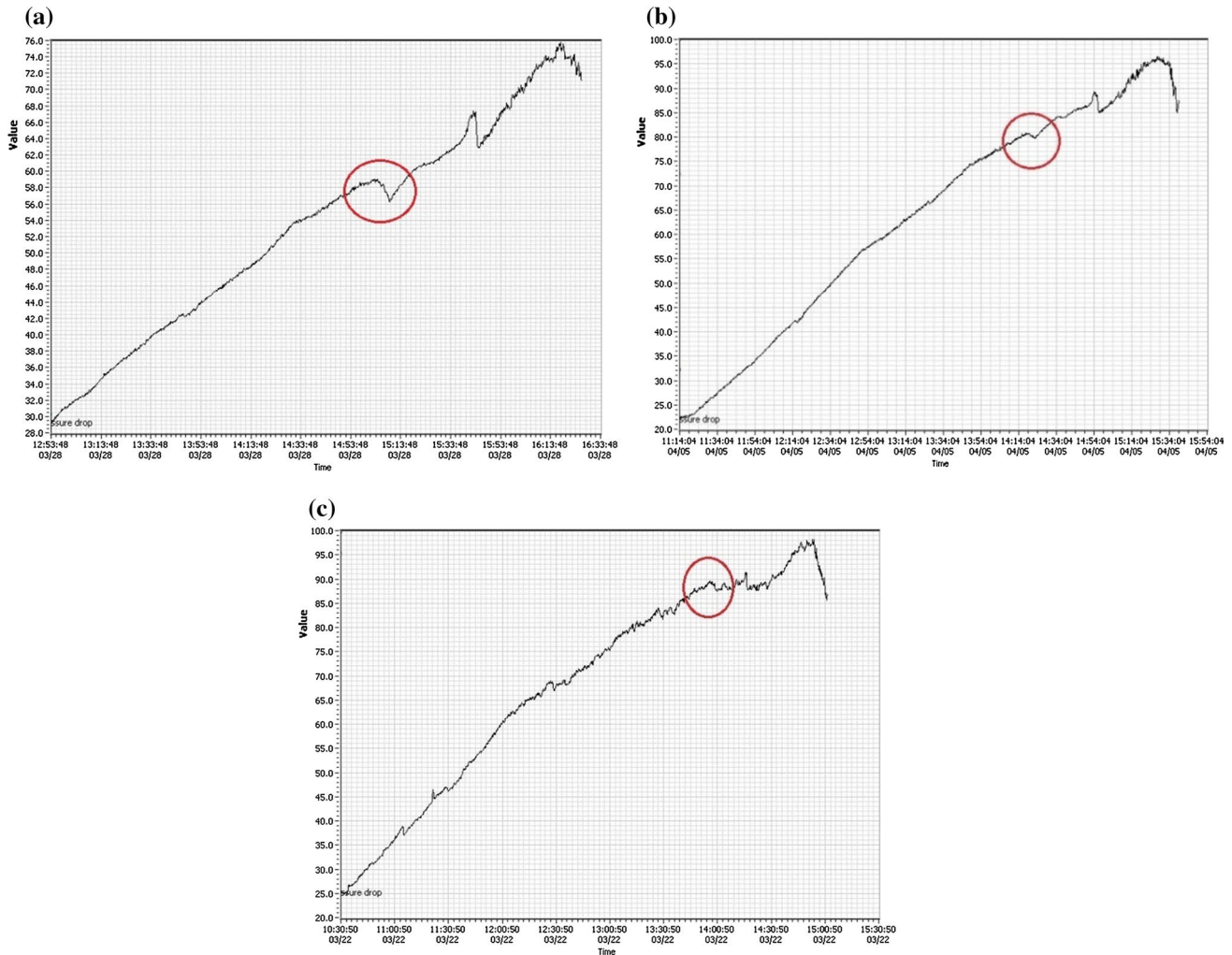

Fig. 9 Fan stall situations **a** Test 1 **b** Test 2 **c** Test 3

ation is consistent with the study performed by Ye et al. [12], which mentions the critical air velocity phenomenon; however, it is quite different in other studies as mentioned in the literature review.

- Considering the fan stall issue, when the limit of pressure drop permitted is exceeded, it could have a detrimental impact on the fan, evaporator and ductwork. Therefore, the starting point of stall could be an optimum point for the running of the defrost process because the half channel area is blocked by frost as mentioned in other studies. In order to detect this situation, other studies on unit coolers considering real fan impacts at different operation conditions have to be carried out.

- As mentioned in the previous sections, initial frost growth could be critical for further frost growth. Although a microscope camera was used in order to see frost shapes depending on the air inlet velocity, the effect of air velocity on initial frost growth was not detected due to the fact that the frost formation occurred at the stabilization period of the test operations.

- Further studies should investigate the effect of subsequent refrosting after a defrost period because the retaining water in the heat exchanger after the defrost operation has a detrimental impact on the change of heat transfer rate of the evaporator and frost growth.

References

1. Chen H, Thomasb L, Besanta RW (2013) Fan supplied heat exchanger fin performance under frosting conditions. Int J Refrig 26:140–149

2. Aljuwayhel NF, Reindl DT, Klein SA, Nellis GF (2008) Experimental investigation of the performance of industrial evaporator coils operating under frosting conditions. Int J Refrig 31:98–106

3. Schmidt EO, Kristensen MS (2014) Optimization of defrost strategy for an air-to-water heat pump-Dynamic modelling and experimental study of frost formation on cross-flow heat exchanger surface. Master Thesis, Aalborg University, Denmark

4. Londero DSD (2012) Frost formation on fan-supplied tube-fin evaporators: a visual and numerical analysis. In: International refrigeration and air conditioning conference. paper 1164, Purdue University, USA

5. Huang JM, Hsieh WC, Ke XJ, Wang CC (2008) The effects of frost thickness on the heat transfer of finned tube heat exchanger subject to the combined influence of fan types. Appl Therm Eng 28:728–737

6. Groll EA, Braun JE, Bach CK (2011) Optimizing refrigerant distribution in Evaporators. Final project report prepared for California Energy Commission, Purdue University, USA

7. Yan WM, Li HY, Wu YJ, Lin JY, Chang WR (2003) Performance of finned tube heat exchangers operating under frosting conditions. Int J Heat Mass Transf 46:871–877

8. Cui J, Li WZ, Liu Y, Zhao YS (2011) A new model for predicting performance of fin-and-tube heat exchanger under frost condition. Int J Heat Fluid Flow 32:249–260

9. Padhmanabhan SK, Fisher DE, Cremaschi L, Moallem E (2011) Modeling non-uniform frost growth on a fin-and-tube heat exchanger. Int J Refrig 34:2018–2030

10. Haijie Q, Weizhong L, Bo D, Zhihai Z, Weiying Z (2014) Experimental study of the characteristic of frosting on low-temperature air cooler. Int J Exp Therm Fluid Sci 55:106–114

11. Tashiro Y, Hamada M (2014) Experimental Evaluation of the Frost Formation. In: International refrigeration and air conditioning conference. Paper 1395, Purdue University, USA

12. Ye HY, Park JS, Lee KS (2014) Frost retardation on fin-tube heat exchangers using mass transfer characteristics with respect to air velocity. Int J Heat Mass Transf 79:689–693

13. Bell S (1999) Measurement good practice guide no.11. A beginner's guide to uncertainty of measurement, technical report. National Physical Laboratory, Teddington, Middlesex, United Kingdom

14. Jansen DD (2013) Experimental strategies for frost analysis. Master Thesis, University of Minnesota, USA